Theoretical Investigation of the ECC Peak for Charged Particles with the CTMC Method

AUTHOR(S):

Tkési, Károly; Mukoyama, Takeshi

CITATION:

Tkési, Károly ...[et al]. Theoretical Investigation of the ECC Peak for Charged Particles with the CTMC Method. Bulletin of the Institute for Chemical Research, Kyoto University 1994, 72(1): 62-68

ISSUE DATE:

1994-03-31

URL:

http://hdl.handle.net/2433/77548

Bull. Inst. Chem. Res., Kyoto Univ., Vol.72, No.1, 1994

Theoretical Investigation of the ECC Peak for Charged Particles with the CTMC Method

Károly TŐKÉSI* and Takeshi MUKOYAMA§

Received February 10, 1994

Using the classical trajectory Monte Carlo (CTMC) method, we have calculated the energy spectra of the target electrons ejected in $p + H^0$ at an impact energy of 25 keV. We have described a simple way to determine the ECC peak with charged particles. This study has shown that the electronic spectrum is very sensitive to the choice of the energy and solid angle windows for the evaluation of the calculated data.

KEY WORDS: Classical trajectory Monte Carlo method / Electron capture to continuum / Electron spectrum

I. INTRODUCTION

Two decades ago Crooks and Rudd[1] first observed a sharp peak in the doubly differential cross section (DDCS) of electrons ejected in ion-atom collisions. This cusp-shaped peak appears close to the direction of the projectile at the energy where the velocity of the ejected electron is equal to that of the projectile. When the projectile is a bare nucleus, the electron comes only from the target atom. In this case, the cusp peak arises due to the process where an atomic electron is dragged by the projectile and moves with it. This process is called the electron capture to the continuum (ECC).

Since the work of Crooks and Rudd,[1] extensive experimental studies on the ECC have been performed to investigate cusp peaks, such as position, shape, intensity, and full width at half maximum (FWHM), as a function of projectile energy for various combinations of projectiles and target atoms.[2-4] Theoretical models for these parameters have also been developed.[5,6]

It is relatively easy to calculate these parameters of the cusp peak for projectiles with low and high velocities because the perturbation theories, such as the Born approximation, can be used. On the other hand, theoretical models are rather scarce in the case of intermediate energy range ($25\ \mathrm{keV/amu} \leq E \leq 500\ \mathrm{keV/amu}$), where the projectile velocity is almost same as the velocity of the electrons moving around the target nucleus. Studies of the ECC peak in this energy region give sensitive theoretical and experimental tests of the collision dynamics between three particles, i.e. projectile, electron, and target nucleus.

In the present work, we use the classical trajectory Monte Carlo (CTMC) method and in-

*Károly Tőkési : Institute of Nuclear Research of the Hungarian Academy of Sciences (ATOMKI), H-4001 Debrecen, Pf. 51, Hungary

§向山 毅 : Division of States and Structures, Institue for Chemical Research, Kyoto University, Uji, Kyoto, 611 Japan

vestigate the cusp peak produced in the reaction

$$p + H^0 \rightarrow p + H^+ + e^-.$$

The Monte Carlo simulation is a non-perturbative method and at the same time a very powerful tool to study ECC peak in the intermediate energy region, where the perturbative treatments are invalid. Moreover, the CTMC method can also provide a physical insight to the ECC process.

It should be noted that the CTMC calculation by Banks *et al.*[7] is in agreement with the coupled-channel calculation of Shakeshaft[6] to predict a large ECC component in the ionization cross section for $H^+ + H$, which has a maximum at $E = 50$ keV. We further note that the earlier CTMC works[8,9] could succeed in calculating the DDCS of the ECC peak when the projectile energy is greater than 37.5 keV. However, for low-energy projectiles the CTMC calculations of the ECC peak are time-consuming because we must trace the projectile and the ejected electron far from the target nucleus. It is hoped to develope a simple method to reduce the computation time to a great extent.

In this paper we present a simple procedure to calculate the DDCS of the ECC peak by the use of the CTMC method and address the problem of the calculating and evaluating procedures. The projectile velocity is chosen at the low impact energy, $E_{projectile} = 25$ keV.

II. THEORETICAL METHOD

In the CTMC approach, the Newton's[10-12] or Hamilton's[13,14] classical non-relativistic equations of motions for the three-body system are solved numerically for a statistically large number of trajectories with initial conditions determined pseudorandomly. In the present study, we use the Newton's equations:

$$m_i \frac{d^2\vec{r}_i}{d^2t} = \sum_{i \neq j} Z_i Z_j \frac{\vec{r}_i - \vec{r}_j}{|\vec{r}_i - \vec{r}_j|^3} \quad (i = 1,2,3), \tag{1}$$

Where m_i, $\vec{r}_i$, and Z_i denote the mass, the position vector, and the charge of the i-th particle, respectively. We consider the three-particle system that the projectile (P), the particle 1, collides with the target atom, the particles 2 and 3. In the initial state, the target consists of a bound system (T_e), where the electron (e), the particle 2, is moving around the target nucleus (T), the particle 3.

The uniform motion of the center of mass of three particles is usually separated out, and the relative motion of the three particles is expressed in terms of their relative positions $\vec{A} = \vec{r}_2 - \vec{r}_3$, $\vec{B} = \vec{r}_3 - \vec{r}_1$, $\vec{C} = \vec{r}_1 - \vec{r}_2$ (see Fig. 1), and the corresponding velocities $\vec{V}_A = \dot{\vec{A}}$, $\vec{V}_B = \dot{\vec{B}}$, $\vec{V}_C = \dot{\vec{C}}$. Here dot means the derivative with respect to the time variable. From the relation between the relative coordinates in the center-of-mass system

$$\vec{A} + \vec{B} + \vec{C} = 0, \tag{2}$$

only two vector equations of motion are independent:

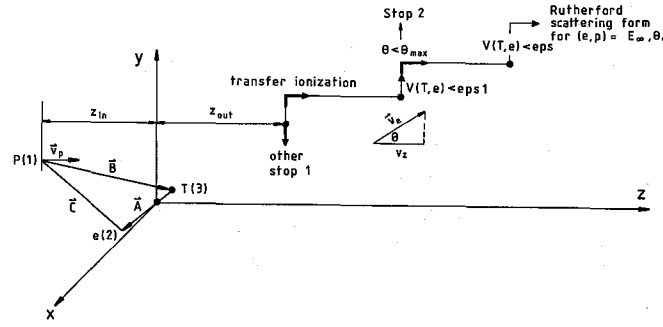

Fig. 1. Schematic diagram of the ECC calculations.

$$\dot{\vec{V}}_A = \left[\frac{(N_2+N_3)Z_2Z_3}{A^3} + \frac{N_2Z_1Z_2}{|A+B|^3}\right]\vec{A} + \left[\frac{N_2Z_1Z_3}{|A+B|^3} - \frac{N_3Z_1Z_3}{B^3}\right]\vec{B}, \tag{3}$$

$$\dot{\vec{V}}_B = \left[\frac{N_3Z_2Z_3}{A^3} + \frac{N_1Z_1Z_2}{|A+B|^3}\right]\vec{A} + \left[-\frac{N_1Z_1Z_2}{|A+B|^3} - \frac{(N_1+N_3)Z_1Z_3}{B^3}\right]\vec{B} \tag{4}$$

with

$$N_i = (m_i)^{-1} \quad (i=1,2,3). \tag{5}$$

These equations are integrated with time as the independent variable by the use of the standard Runge-Kutta method. The initial conditions, such as the impact parameter of particle 1 (projectile) with respect to the target system (nucleus plus electron) and the orientation and velocity of the particle 2 (electron) moving around the particle 3 (target nucleus), are selected using random numbers. These parameters were chosen at a relatively large distance between the projectile and target atom (Z_{in} in Fig. 1).

As a result of the integration (Z_{out} in Fig. 1), we consider four final exit channels: direct process, direct ionization, transfer ionization, and charge transfer. The direct channel consists of the elastic scattering of the projectile and the excitation process of the target atom. The direct ionization channel corresponds to the case where the target electron is ejected but its interaction with the target nucleus is stronger than with the projectile. On the contrary, in the transfer ionization the ejected electron has stronger interaction with the projectile than with the target nucleus. In the case of the charge transfer process, the target electron is captured into an unoccupied bound state of the projectile. These final sates are determined by testing the values of relative positions, directions of relative velocities, the center-of-mass energy of the projectile-electron system (E_{P_e}), and that of the target-electron system (E_{T_e}). The test conditions for the final states are shown in Table I.

The total cross sections for a specific event (CH) are calculated by

$$\sigma_{CH} = \frac{2\pi b_{max}\Sigma b_i}{N}. \tag{6}$$

The DDCS is obtained in the following form:

Table I. Test conditions for the final states. A plus sign means that the test must be passed, a minus sign that it must not be passed, and a zero that it is not made. The entries and quantities are defined as follows: D: = direct (elastic scattering or excitation), DI: = direct ionization, TI: = transfer ionization (ECC), CT: = charge transfer (EC), E_{P_e}: = centre-of-mass energy of (P_e) at time t $(+\infty)$, E_{T_e}: = centre-of-mass energy of (T_e) at time t $(+\infty)$, E_{TP}: = centre-of-mass energy of (TP) at time t $(+\infty)$, $\vec{A}$, $\vec{B}$, $\vec{C}$ relative positions of three particles, $\vec{V}_A$, $\vec{V}_B$, $\vec{V}_C$ relative velocities of three particles, U: = total potential energy of the electron in the total field of particles P and T, U_0: = maximum value of U.

Test	D	DI	TI	CT
$A < C$	0	+	−	0
$E_{P_e} > 0$	+	+	+	0
$E_{T_e} > 0$	0	+	+	+
$E_{P_e} < U_0$	0	0	0	+
$E_{T_e} < U_0$	+	0	0	0
$\vec{A}\ \vec{V}_A$	0	+	+	0
$\vec{B}\ \vec{V}_B$	+	0	0	+
$\vec{C}\ \vec{V}_C$	0	+	+	0
$B < A$	0	0	0	0

$$\frac{d^2\sigma_{CH}}{dE\,d\Omega} = \frac{b_{max}\sum b_i}{N(\cos\vartheta_{min} - \cos\vartheta_{max})\,\Delta E} \tag{7}$$

The standard deviation of the cross section shown above is given by

$$\Delta X = X\left(\frac{N - N_X}{NN_X}\right)^{1/2}, \tag{8}$$

where X denotes σ_{CH} or DDCS.

In Eqs. (6), (7), and (8), N is the total number of trajectories calculated for impact parameters less than b_{max}, and N_{CH} is the number of trajectories that satisfy the criteria for a given collision process such as capture, ionization, and excitation, b_i is the actual impact parameter when the actual criteria is given, ΔE is the energy window and $2\pi(\cos\vartheta_{min} - \cos\vartheta_{max})$ is the solid angle window.

III. COMPUTATIONAL PROCEDURES

The equations (3) are (4) and used to calculate the impact ionization cross section for 25-keV protons on hydrogen. Throughout all the calculations in the present work atomic units are used.

Since the ECC peak is caused by the Coulomb force and this is the long range force, it is sometimes necessary to integrate the equation of motion over 10^6 au. Because of the limited

computation time we applied a simple way of the integration, as described below. In Fig. 1, the schematic diagram of the integration procedures is shown.

First, we integrate the equation of motion so far the real exit channel is observed (elastic scattering or excitation, direct ionization, transfer ionization, charge transfer) . This point is the so-called big turning point, because we continue the integration only if the exit channel is the transfer ionization and stop it for all other cases (Stop 1 point in Fig. 1). It should be noted that before this calculation we checked the exit channel of the direct ionization too, but neglected the latter because this channel was found not to cause the ECC event.

After the first turning point, we change to another time integration step. Usually the optimum size of the new step was chosen to be $8 \div 10$ times larger than the previous step size. It is possible to use larger step size because after this point we have three free particles.

The second turning point is chosen to be approximately 10^4 au from the colliding center. There we are rather at long distance from the target nucleus and the interaction between the ejected electron and the target nucleus is less than *eps*1 (10^{-4} au). At this point we estimate the critical angle (Θ_{max}), shown in the Fig. 1, for the ionized electron. If the angular deflection of the ejected electron is less than Θ_{max}, the electron is considered to be the ECC electron, but not in all other cases and stop the integration of equation of motions (Stop 2 point in Fig. 1).

In the next step, we integrate the equation of motion until the interaction between the ionized electron and the target nucleus becomes less than *eps* (10^{-6}). This is a *normal* exit. When the distance between the projectile and the target nucleus is greater than B_{finish} (several times larger than $1/eps$), we stop the integration, too. This case corresponds to the *abnormal* exit. In the latter case the interaction between the ejected electron and the target nucleus is in order of 10^{-5} au. This exit test is necessary because there are so extreme trajectoris that the earlier exit test is not useful. The real integration procedure is stopped at this point. Then we introduce the final approximation as follows: We neglected the interaction between the electron and the target nucleus (this is less than 10^{-6} au) and use the Rutherford scattering formula between the ionized electron and the projectile to define the energy and deflection angle of the ejected electron at the infinite time.

IV. RESULTS AND DISCUSSION

All the numerical computations in the present work have been performed on the CRAY Y-MP2E supercomputer in the Institute for Chemical Research, Kyoto University.

As has been described above, it was found that in the present case the ECC peak arises due to the transfer ionization process and the direct ionization mechanism plays a minor role. Therefore we traced only the transfer ionization channel and neglected the contributions from the direct ionization process.

The calculated results of the DDCS for the 25-keV protons on hydrogen is shown in Fig. 2. The total number of histories was 2×10^6. When the projectile energy is 25 keV and the ejected electron spectrum is observed at $0.2°$, the solid angle window becomes 0.4 sr and the energy window is 0.22 eV. It is clear from the figure that the calculated shape of the ECC peak is similar to the shape observed by Dahl[15] and by Gibson and Reid[16] for 100-keV protons on He.

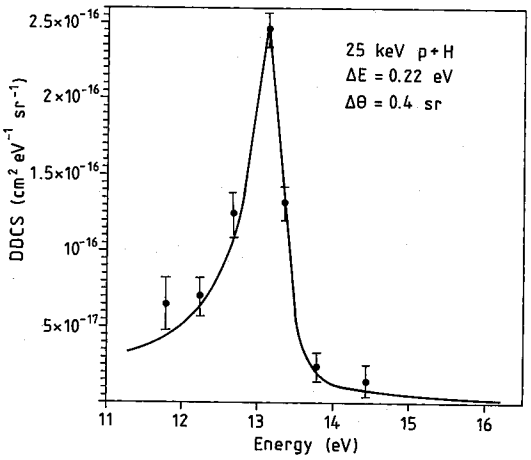

Fig. 2. Calculated shape of the ECC peak in the case of 25 keV $p + H^0$ collisions. The energy window is set to 0.22 eV and the solid angle window is 0.4 sr.

Since it is well known that the peak position of the ECC sharply depends on the observed angle and the CTMC method can be considered as a kind of theoretical experiment, we tested the evaluation procedure of the data. We change the energy and solid-angle windows, see Table II, and computed the position of the cusp peak (E).

In our calculations the energy of projectile was 25 keV and the cusp peak should appear at $E_e = 13.5$ eV. When a large step size is used for the energy and solid-angle windows, the CTMC calculation gives smaller peak energy and the difference between the calculated peak position and the expected energy is significant, as large as 1 eV. This difference decreases with decreasing the size of the energy and solid-angle windows.

For small solid-angle windows, the calculated cusp peak position reduces to the expected energy quickly even with large energy windows. When the solid angle window is rather small (0.4 sr), the difference sharply depended on the size of the energy window. At the fixed number of the events (12847), we could get the best value for $\Delta E = 0.22$ eV and $\Delta\Omega = 0.4$ sr. In this case the calculated cusp peak position was 13.4 eV. We can expect that a better agreement between the calculated and expected energies be obtained if we use more trajectories.

Table II. Calculated dependence of peak position on the energy and solid-angle windows.

ΔE (ev)	$\Delta\Theta$ (sr)	Peak position (ev)
1.0	1.0	12.5
1.0	0.8	12.8
0.44	0.8	13.0
0.44	0.4	13.2
0.22	0.4	13.4

V. CONCLUSION

In the present work, we have calculated the ECC peak by the CTMC method. We have shown that the ECC electrons are coming only from the transfer ionization process. It is interesing to note that we described the transfer ionization process over 40 au from the collision center. However, since the Coulomb force is a long range force, the effect of this force cannot be neglected until $10^4 \div 10^5$ au.

We described that the position of the ECC peak (E) strongly depends on the evaluation procedure, i.e. if we decrease the solid angle or energy windows, then it moves to E_e.

The present calculation method can reduce the total CPU time by about 50% in comparison with the conventional methods. This fact indicates that the present method is very useful to calculate the ECC peak in ion-atom collisions because this type of calculations require several billion trajectories.

ACKNOWLEDGEMENTS

This work was performed under the Japanese-Hungarian Cooperative Research Project. We would like to acknowledge the Japan Society for Promotion of Science and the Hungarian Academy of Sciences for their support. Computation time in the present work was provided by the Supercomputer Laboratory, Institute for Chemical Research, Kyoto University.

REFERENCES

(1) G. B. Crooks and M. E. Rudd, *Phys. Rev. Lett.*, **25**, 1599 (1970).
(2) M. Breinig, S. B. Elston, S. Huldt, L. Liljebly, C. R. Vane, S. D. Berry, G. A. Glass, M. Schauer, I. A. Sellin, G. D. Alton, S. Datz, S. Overbury, R. Laubert, and M. Sutter, *Phys. Rev. A*, **25**, 3015 (1982).
(3) A. Kövér, L. Sarkadi, J. Pálinkás, D. Berényi, Gy. Szabó, T. Vajnai, O. Heil, K. O. Groeneveld, J. Gibons, and I. A. Sellin, *J. Phys. B: At. Mol. Opt. Phys.*, **22**, 1595 (1989).
(4) L. Sarkadi, J. Pálinkás, A. Kövér, D. Berényi, and T. Vajnai, *Phys. Rev. Lett.*, **62** 527 (1989).
(5) J. Macek, *Phys. Rev. A*, **1**, 235 (1970).
(6) R. Shakeshaft, *Phys. Rev. A*, **18**, 1930 (1978).
(7) D. Banks, K. S. Barnes, and J. Mc. B. Wilson, *J. Phys. B: At. Mol. Phys.*, **9**, L141 (1976).
(8) R. E. Olson, *Phys. Rev. A*, **27**, 1871 (1983).
(9) C. O. Reinhold and D. R. Schultz, *J. Phys. B: At. Mol. Opt. Phys.*, **22**, L565 (1989).
(10) R. Abrines and I. C. Percival, *Proc. Phys. Soc. (London)*, **8**, 861 (1966).
(11) G. Schiwietz and W. Fritsch, *J. Phys. B: At. Mol. Opt. Phys.*, **20**, 5463 (1987).
(12) K. Tőkési and G. Hock, *ATOMKI Ann. Rep.*, **1989**, 49 (1990).
(13) R. E. Olson and A. Salop, *Phys. Rev. A*, **16**, 531 (1977).
(14) J. S. Cohen, *Phys. Rev. A*, **26**, 3008 (1982).
(15) P. Dahl, *J. Phys. B: At. Mol. Phys.*, **18**, 1181 (1985).
(16) D. K. Gibson and I. B. Reid, *J. Phys. B: At. Mol. Phys.*, **19**, 3265 (1986).